# Numerical Evaluation of the Aerodynamic Performance of U-shape Building Section: Comparisons between Different Simulations

W. A. Aissa* and I. K. Mohamed

Faculty of Engineering at Rabigh, King Abdulaziz University, KSA
Permanent address: Mech. Power Dept., Faculty of Energy Engineering, Aswan University, Aswan, Egypt
*E-mail: walidaniss@gmail.com

**Abstract:** Numerical studies of flow around typical elements of the urban canopy [isolated (rectangular, U-shape,) buildings, groups of buildings, street canyons] could provide valuable substitutes for field data sets. Computational Fluid Dynamics is utilized to analyze the aerodynamic performance of U-shape building section. Realizable $k$-$\varepsilon$ turbulence model is used to quantify the shape factor for a specific range of Reynolds number (varying from $6.8116 \times 10^4$ to $3.4058 \times 10^5$) and for both cases of steady and unsteady states at 0° wind angle. Pressure factor distribution is plotted for different elements of the section under investigation for different boundary conditions and different values of Reynolds number. The corresponding shape factors for different simulations are tabulated. Computed values of shape factor for different simulations are compared with the corresponding values listed in the literature. It is shown that current investigation of unsteady flow at Reynolds number of $2.724644 \times 10^5$ presents the closest results to GB code in terms of shape factor. The asymmetry of the flow field and vortex structure for zero wind angleis discussed.

[W. A. Aissa and I. K. Mohamed. **Numerical Evaluation of the Aerodynamic Performance of U-shape Building Section: Comparisons between Different Simulations.** *Life Sci J* 2013;10(3):2684-2690]. (ISSN: 1097-8135). http://www.lifescienceite.com. 387

**Keywords:** Turbulence model; Numerical investigation; Aerodynamic performance; U-section

## 1. Introduction

The civil engineering construction recently tends to be huge, large-span, higher and lighter (Yuan, Zhou, Yao and Xie, 2012). Hence, it should have higher flexibility, lower natural vibration frequency and more sensitivity to wind loads. The loading code of every country can be used to evaluate the shape factor of regular rectangular section. The absence of corresponding tabulations for complex sections implies making research to evaluate their aerodynamic performance.

Experimental investigation (Blocken, Stathopoulos, Saathoff and Wang, 2008) and (Lien, Yee, and Cheng, 2004); is expensive and time consuming. High revolution advance in computing hardware and numerical techniques (Lien , Yee, and Cheng, 2004)and (Chang and Meroney, 2003);made the numerical investigation of flow around isolated structures or single buildings to be more reliable. The development of theory of Computational Fluid Dynamics (CFD), hardware and the computer's software enables efficient simulation of large numbers of discrete bluff obstacles (e.g., buildings, trees, and other obstructions in a prescribed domain)(Lien , Yee, and Cheng, 2004);and its impact on the atmospheric boundary-layer flow is a very important task.

The flow patterns that develop around specific building (Chang and Meroney, 2003), (Leitl, Kastner-Klein, Rau and Meroney, 1997) & (Chang and Meroney, 2001) govern the wind forces on the building, the distribution of pressure about the building and pollution about the building and its wake.

Yuan, Zhou, Yao and Xie (2012) adopted Standard $k$-$\varepsilon$ and Realizable $k$-$\varepsilon$ turbulence models to investigate the aerodynamic performance of concave building section. They determined the shape factor of the section for different wind angles and compared the computed values with standard values in order to explore the applicability of turbulence models for numerical simulation around blunt body, and analyze the structure of flow field. They stated that Realizable $k$-$\varepsilon$ model can capture the unsteady flow characteristics of flow around the blunt body better.

Leitl, Kastner-Klein, Rau and Meroney (1997) considered the flow and dispersion of gases emitted by point sources located near a U-shaped building which were determined by the prognostic model FLUENT using the renormalized-group- theory (RNG) version of the $k$-$\varepsilon$ turbulent closure approximation. They compared their calculations against detailed wind tunnel measurements and an array of other numerical predictions and concluded that the utilized model led to improved predictions of flow and separation around bluff bodies.
He and Song (1996) carried out a numerical study of wind flow around the TTU building and the roof corner vortex using an advanced CFD method with large eddy simulation approach to explore a deeper insight into the physical nature of the flow characteristics.

Moroney, Leitl, Rafailidis and Schatzmann (1999) validated the commercial codes FLUENT and FLUENT/UNS for air-pollution aerodynamics exercise to four sets of wind-tunnel data representing measurements of flow around bluff generic shape model buildings in simulated atmospheric shear layers.

It was revealed in (Blocken, Stathopoulos, Saathoff and Wang, 2008) and (Chang and Meroney, 2003); that transient simulations might be required to achieve more accurate results. Further, it was indicated in (Chang and Meroney, 2001); that "quantitative" equivalence between numerical and experimental data of pressures over a bluff body will occur only if careful attention is paid to inlet profiles, grid adaptation and the turbulent model chosen.

It was mentioned in (Kastner-Klein and Plate, 1997); that the atmospheric surface layer can be modeled as a horizontally-homogeneous turbulent boundary layer, which is one with constant properties in directions tangential to the ground and hence the only variation is along the vertical axis. Further, it was stated in (Norris and Richards, 2010); that the flow within the computational domain is driven by a shear stress at the top boundary.

In this paper, FLUENT of CFD simulations are performed in an attempt to analyze the aerodynamic performance of U-shape building section, evaluate the shape factors for its different elements and analyze the development of the construction wake flow. In addition, the shape factors for different elements of U-shape building section at zero wind angle and different values of Reynolds number and computation parameters are compared with those of Yuan, Zhou, Yao and Xie (2012); to explore the numerical simulation of flow around blunt body.

## 2. Physical Model

The study used a basic building shape, utilized in **(**Yuan, Zhou, Yao and Xie, 2012**).** The physical dimensions and name of each element in the building section are shown in figure1 (a) and figure 1(b) respectively.

The dimensional scale is *B1*: *B2*: *L1*: *L2*: *L3* = 1.0: 1.2: 1.0: 1.7: 1.0. Wind approaches the section as illustrated in figure 1(a). Hence, the section is up-down symmetrical. Reynolds number taken to confirm with real construction wind flow is *Re*, where, $Re = \rho u D/\mu$, where $\rho$is the air density (=1.225 kg/m$^3$), $\mu$ is the air dynamic viscosity coefficient (=1.7894×10$^{-5}$kg/(m.s)) and *D* is the scale feature of the section. In this study, *D* is taken as the sum of *L1*, *L2* and *L3* and is taken as unity; *u* is the incoming wind speed. Range of *u* utilized in this study is 1 m/s to 5 m/s resulting in Reynolds number ranging from 6.81161×10$^4$to 3.4058 ×10$^5$.

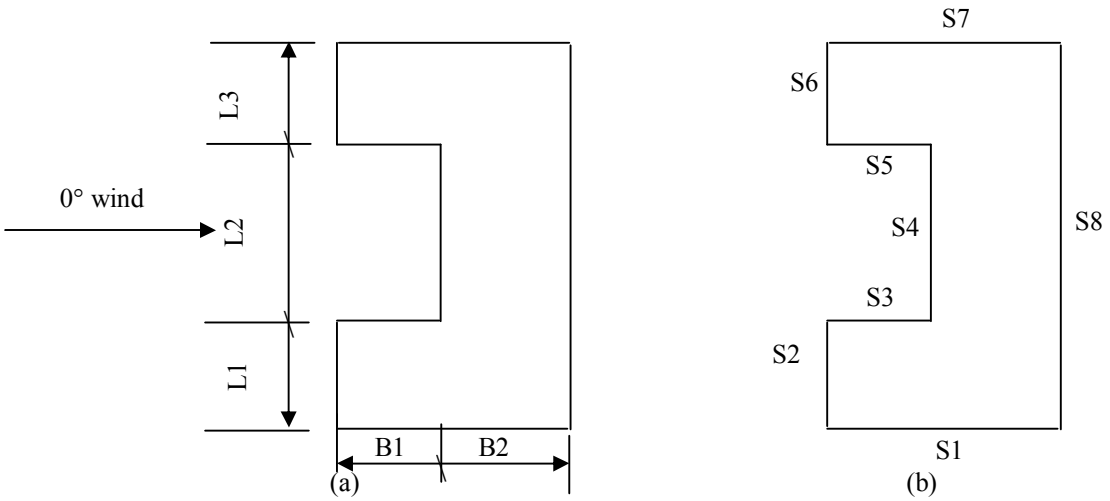


Figure 1. Physical Dimensions and Name of Each Element of the Cross Section.

## 3. Numerical Analysis

### 3.1. Turbulence Model

Version 6.3.26 of the FLUENT code and version 2.3.16 of GAMBIT grid generation code are used for numerical simulations. The code was run on an Intel® Core™ CPU@2.40GHz using a Microsoft Windows 7 Enterprise Operating System to numerically simulate the aerodynamic performance of U-shape building section using Realizable *k*-$\varepsilon$as a turbulence model in the current investigation with the constants of $C_2$ = 1.9; $\sigma_k$ = 1.0; $\sigma_\varepsilon$ = 1.2. Reynolds average equation is obtained by doing ensemble average to standard Navier-Stokes equation. The momentum and continuity equations are:

$$\frac{\partial \langle u_j \rangle}{\partial t} + \langle u_i \rangle \frac{\partial \langle u_i \rangle}{\partial x_j} = -\frac{1}{\rho}\frac{\partial \langle P \rangle}{\partial x_i} + \frac{\partial}{\partial x_i}\left[\vartheta \frac{\partial \langle u_i \rangle}{\partial x_j} - \langle u_i u_j \rangle\right] \quad (1)$$

$$\frac{\partial(u_i)}{\partial x_i} = 0 \quad (2)$$

where, $\langle u_i \rangle$ ($i$ = 1,2,3) representing average velocity component $X$, $Y$, $Z$, $\langle P \rangle$ is the average pressure, $\nu$ is the air dynamic viscosity coefficient, $\rho$ is the air density.- $\rho\langle u_i u_j \rangle$ is the Reynolds stress which lead the equation unseal.

### 3.2. Mesh Model

A schematic of the whole calculation field used for the current investigation is shown in figure 2. The size of the whole calculation field; which is rectangular area, is $20D \times 40D$, $D$ is the scale feature of the section. The field extended $9.5D$ and $29.5D$ upstream and downstream of the section respectively. Each of the two valleys of the section horizontal direction is 9.5 $D$. It should be expected that the gradient change nearby the section area is great. Quadrilateral mesh is utilized for the entire area in the current investigation; Figure2.The mesh size is $D$/200. The number of mesh within the entire area is 346,568.

### 3.3. Boundary Conditions

The setting of boundary conditions are: (1) Entrance boundary adopts the speed inlet condition, preset inlet wind speed and incoming flow direction; (2) Exit boundary adopts pressure-outlet condition, zero static pressure is set; (3) Set the wall of section as no slip wall. Runs are done for two boundary conditions; Condition 1 and Condition 2, which correspond to different values of turbulence intensity and viscosity ratio.

### 3.4. Solving Methodology

The unsteady algorithm is adopted, the time step is set at 0.001s, and each working condition calculation time is 5s. SIMPLEC algorithmic is adapted to pressure and velocity coupling. Upon calculating the momentum, turbulence and dissipation rate, second order upwind scheme is used. Calculation is considered convergent, when iteration residual is less than $10^{-6}$.

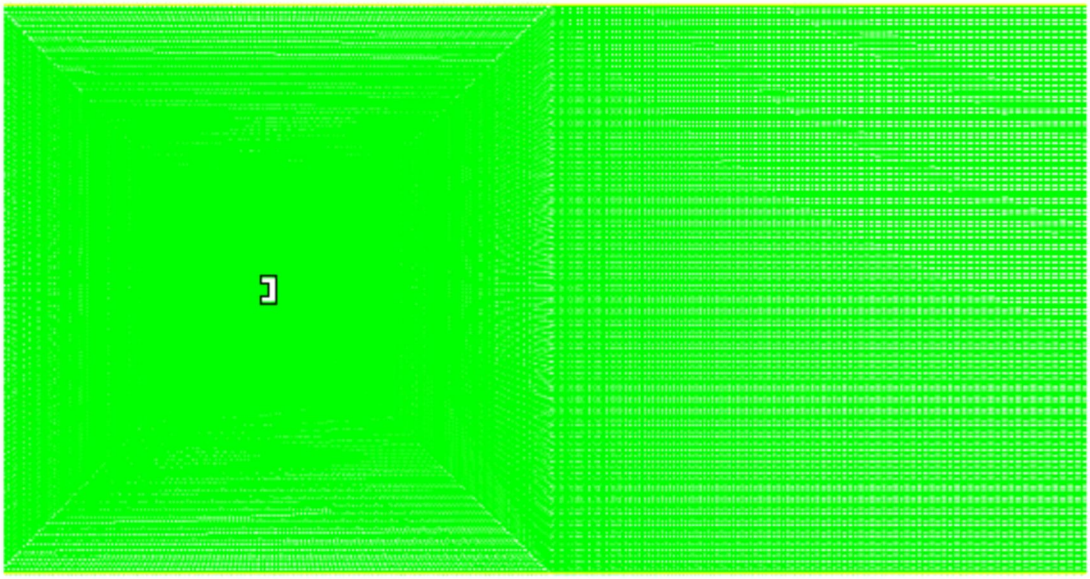

Figure 2.Computational Grid Superimposed on the Flow Domain Used for the Numerical Simulation of the Entire Calculation Field.

## 4. Results

This research analyzes the aerodynamic performance in terms of flow field structure and section shape factor at zero wind angles, for different values of incoming flow wind speed (Reynolds number).

The wind field static pressure distribution around the construction greatly affects the wind resistance of the construction structure. The pressure factor is expressed in non-dimensional form as:

$$C_{Pi} = \frac{P_i}{\frac{1}{2}\rho u^2} \quad (3)$$

where, $P_I$ is the static pressure of element $i$, $\rho$ is the air density, $u$ is the incoming flow wind speed. However, pressure factor is inconvenient at technical application. Usually, shape factor is preferable. Shape factor is defined as the weighted average of pressure factor to area:

$$\mu_i = \frac{\sum_i C_{pi} A_i}{A} \quad (4)$$

where, $A_i$is the area of the i[th] element. $A$ is the sum of the areas of all elements. As the research adopts unsteady algorithm to do the calculation, it is necessary to do time average to shape factor gained by calculation at each moment. Figure 3 presents sample pressure coefficients distribution of different elements of U-section for 4 m/s incoming unsteady state-flow wind speed ($Re = 2.724644\times10^5$) and Condition 1.

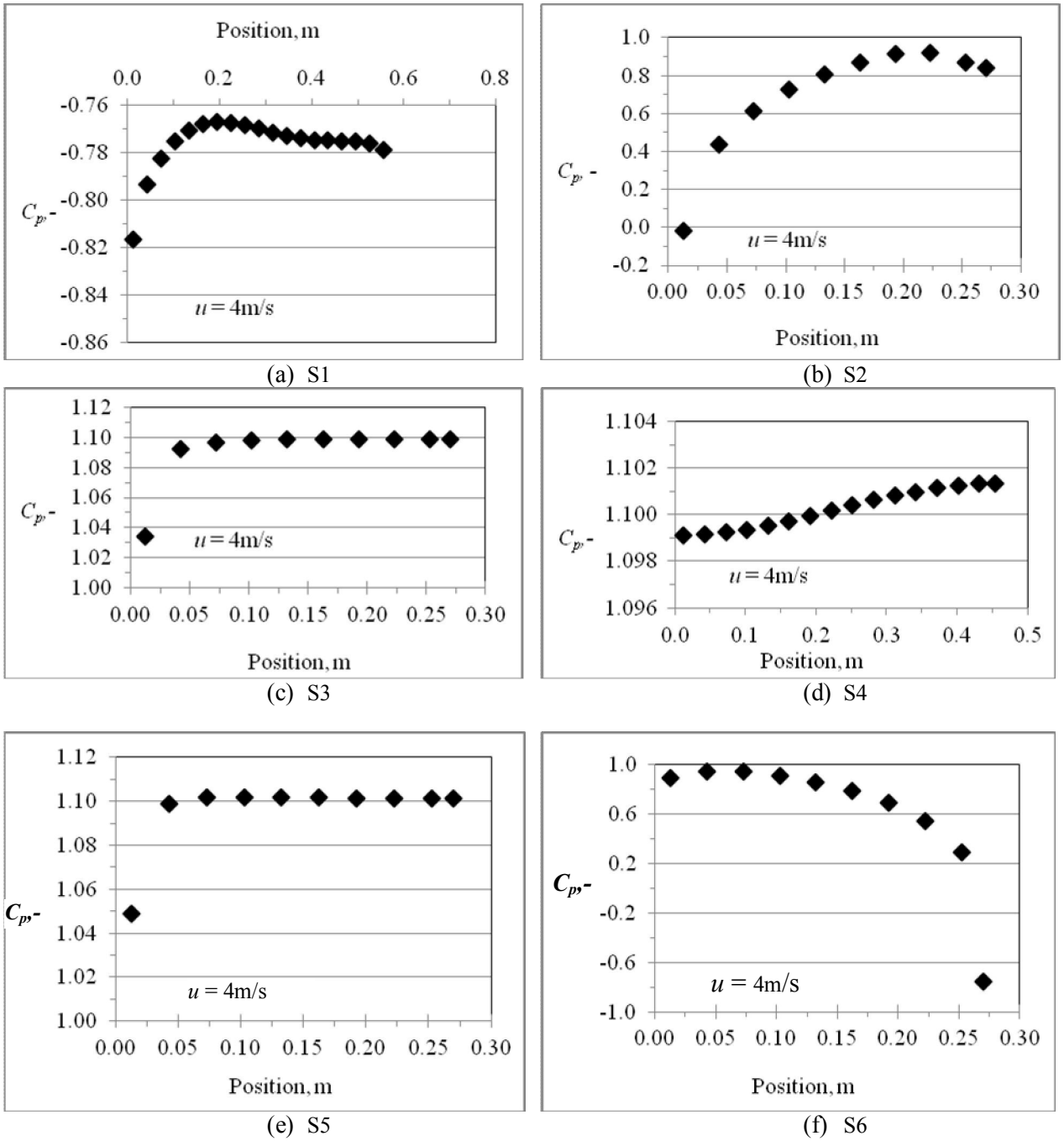


Figure 3. Pressure Coefficients Distribution of Different Elements of the Cross Section at Zero Wind Angle, Unsteady State, $t$ = 5s, $u$ = 4 m/s ($Re = 2.724644\times10^5$) and Condition 1. (Continued)

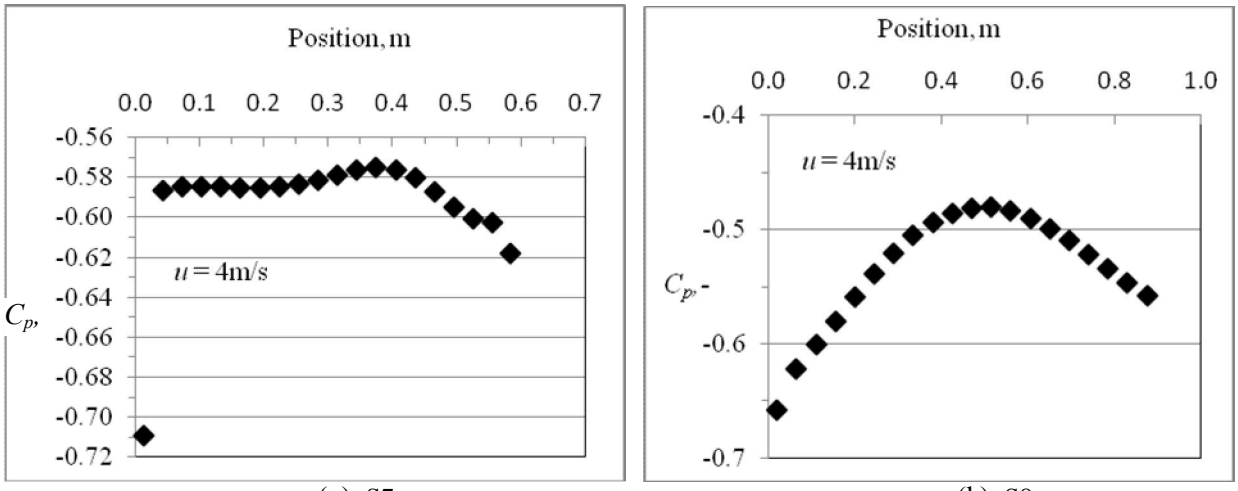


(g) S7 (h) S8

Figure 3. Pressure Coefficients Distribution of Different Elements of the Cross Section at Zero Wind Angle, Unsteady State, $t$ = 5s, $u$ = 4 m/s ($Re$ = 2.724644×10$^5$) and Condition 1. (Concluded)

Specifically, it is anticipated that the pressure coefficient will be large for the front elements of the section in the upstream direction where the incident flow first impinges. This matches the findings listed in (Lien, Yee, and Cheng, 2004). Further, it may be remarked from figure 3 that maximum calculated pressure coefficients, $C_p$ of front, back and top (or bottom) elements of U-section are about 1.101, -0.658, and-0.817, respectively.

Figure 4 illustrates flow line distribution diagram of the section at the same moment and same conditions of figure 3.

In the present case, the impingement process occurring in front of the section provokes a severe concave (unstable) flow curvature in the region of the flow immediately upstream of the section. It can be observed that the sheared velocity profile turns partially upward in the upper part, while the second part turns downward in the lower half. The flow detaches from the downwind edge of the section forming the separation and recirculation flow zone. This profile form is a residue of the strong shear or mixing layer that detaches from the section and spreads outward by pressure or turbulent diffusion. Further, it may be remarked that the vortices shed from both up and down walls and shed downstream of the section. Further, it is may be visible from figure 4, there is no obviously vortex structure inside the Sunken face. This may be attributed that there is no obviously negative pressure distribution inside the Sunken face (the elements S3, S4 and S5); Figure 3, so it can't lead to the separation of the flow field boundary.

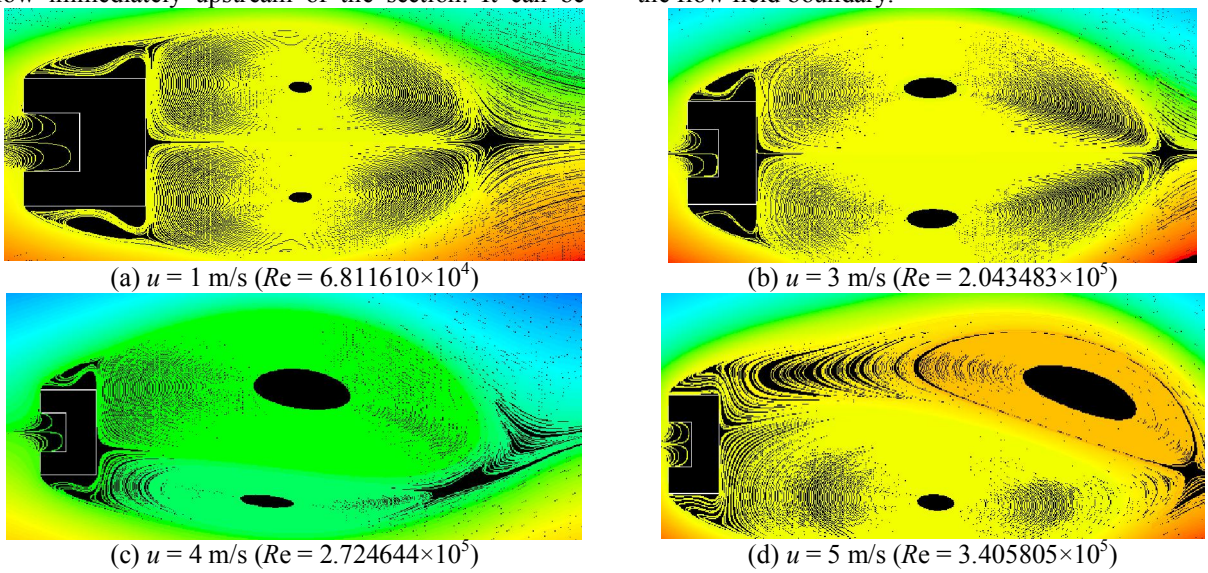

(a) $u$ = 1 m/s ($Re$ = 6.811610×10$^4$) (b) $u$ = 3 m/s ($Re$ = 2.043483×10$^5$)

(c) $u$ = 4 m/s ($Re$ = 2.724644×10$^5$) (d) $u$ = 5 m/s ($Re$ = 3.405805×10$^5$)

Figure 4. Section's Flow Line Distribution Diagram atZero Wind Angle, Unsteady State, $t$ = 5s and Condition 1.

It may be remarked from figure 4 that separation and re-circulation over the front U-building section occurred for all values of Reynolds number under investigation. Further, it may be remarked that for the same time, the position corresponds to the center of the separation bubble increases with increasing the oncoming velocity.

It was indicated in (Yuan, Zhou, Yao and Xie, 2012) that the flow is up-down unsymmetrical because the research adapted unsteady algorithm. However, figure 4 (a) & (b) indicate that the flow is up-down symmetrical for low incoming velocity (Reynolds number) and the vorticity generated on the two sides of the cylinder are similar although the research adapts unsteady algorithm. The up-down asymmetry appears upon increasing the incoming velocity; Figure 4 (c) & (d). This may attributed to the difference between the velocities on the high-and low-velocity sides of the flow. With increase in velocity difference, the strength and depth of the boundary layer, and then the vorticity generated in the separated shear layer on the two sides differ. This possibly creates differences in vortex shedding behavior on the two sides.

Table 1 lists shape factors for different elements of U-shape building section tabulated in GB code at zero wind angles (Yuan, Zhou, Yao and Xie, 2012).

Table 1. Shape Factors for Different Elements of U-shape Building Section Tabulated in GB Code at Zero Wind Angles (Yuan, Zhou, Yao and Xie, 2012).

| | S1 | S2 | S3 | S4 | S5 | S6 | S7 |
|---|---|---|---|---|---|---|---|
| GB | 0.8 | 0.9 | 0.9 | 0.9 | 0.8 | - | - |

Table 2 lists average percentage difference of shape factors for different elements of U-shape building section at zero wind angles for the current investigation and those of Yuan, Zhou, Yao and Xie, (2012).

It may be remarked that Avg. % Difference is sensitive to simulation model, Reynolds number and the state of the flow (steady or unsteady). In addition, it may be noticed that current investigation of unsteady flow at Reynolds number of $2.724644\times10^5$, Condition 1 presents the lowest Avg. % Difference compared to GB code. Further, it may be remarked from table 2 that the elements S1, S5 and S6 have the closest values of shape factors to those of GB code.

Table 2. Avg. % Difference of Shape Factors for Different Elements of U-shapeBuilding Section at Zero Wind Angle for the Current Investigation and those of Yuan, Zhou, Yao and Xie, (2012). (Continued)

| | S1 | S2 | S3 | S4 | S5 | S6 | S7 | S8 | Avg. % Difference |
|---|---|---|---|---|---|---|---|---|---|
| *K-ε, Yuan et al.,*[1]. | 1.25 | 28.89 | 27.78 | 28.89 | 1.25 | 121.43 | 106 | 117.14 | 54.08 |
| *RNG K-ε, Yuan et al.,* [1]. | 13.75 | 24.44 | 23.33 | 24.44 | 13.75 | 85.71 | 116 | 81.43 | 47.86 |
| Current investigation, Steady, Re = $6.81161\times 10^4$ | 0 | 20 | 37.78 | 36.67 | 56.25 | 2.86 | 56 | 14.29 | 27.98 |
| Current investigation, Steady,*Re* =$2.04348\times10^5$, | 1.25 | 25.55 | 15.5 | 15.56 | 30 | 10 | 58 | 2.86 | 19.85 |
| Current investigation, Steady, *Re* = $3.40580\times 10^5$, | 98.75 | 36.67 | 21.11 | 24.44 | 15 | 15.71 | 178 | 27.14 | 52.10 |
| Current investigation, Unsteady, *Re* = $6.81161\times10^4$, Condition1, | 3.75 | 55.55 | 22.22 | 21.11 | 12.5 | 47.14 | 54 | 21.43 | 30 |
| Current investigation, Unsteady, *Re* = $6.81161\times10^4$, Condition1, | 60 | 61.11 | 17.78 | 16.67 | 7.5 | 57.14 | 156 | 8.57 | 48.10 |
| Current investigation, Unsteady, *Re* = $6.81161\times10^4$, Condition2, | 163.75 | 27.78 | 27.78 | 27.78 | 43.75 | 15.71 | 156 | 30 | 61.57 |
| Current investigation, Unsteady, *Re* = $6.81161\times10^4$, Condition2, | 60 | 37.78 | 34.44 | 35.56 | 51.25 | 31.43 | 322 | 47.14 | 77.45 |
| Current investigation Unsteady, *Re* =$2.04348\times10^5$, Condition1, | 13.75 | 21.11 | 22.22 | 23.33 | 36.25 | 5.71 | 40 | 38.57 | 25.12 |
| Current investigation Unsteady, *Re* =$2.04348\times10^5$, Condition1, | 65 | 27.78 | 26.67 | 27.78 | 41.25 | 15.71 | 164 | 1.43 | 46.20 |
| Current investigation, Unsteady, *Re* = $2.04348\times 10^5$, Condition2, | 12.5 | 21.11 | 22.22 | 23.33 | 37.5 | 5.71 | 44 | 34.29 | 25.08 |

Table 2. Avg. % Difference of Shape Factors for Different Elements of U-shape Building Section at Zero Wind Angle for the Current Investigation and those of Yuan, Zhou, Yao and Xie, (2012). (Concluded)

| | S1 | S2 | S3 | S4 | S5 | S6 | S7 | S8 | Avg. % Difference |
|---|---|---|---|---|---|---|---|---|---|
| Current investigation Unsteady, $Re = 2.04348\times 10^5$, Condition2, Avg, | 65 | 27.78 | 26.67 | 27.78 | 42.5 | 15.71 | 166 | 2.86 | 46.79 |
| Current investigation Unsteady, $Re = 2.72464\times10^5$, Condition1, | 2.5 | 24.44 | 21.11 | 22.22 | 37.5 | 1.43 | 18 | 22.86 | 18.76 |
| Current investigation Unsteady, $Re = 2.72464\times10^5$, Condition1, Avg, | 7.5 | 22.22 | 21.11 | 22.22 | 37.5 | 4.29 | 32 | 20 | 20.86 |
| Current investigation Unsteady, $Re = 3.40580\times10^5$, Condition1, | 11.25 | 22.22 | 21.11 | 22.22 | 36.25 | 7.14 | 52 | 10 | 22.77 |
| Current investigation Unsteady, $Re = 3.40580\times10^5$, Condition1, Avg, | 35 | 25.56 | 25.56 | 25.56 | 41.25 | 11.43 | 116 | 7.14 | 35.94 |
| Current investigation Unsteady, $Re = 3.40580\times10^5$, Condition2, | 11.25 | 22.22 | 21.11 | 22.22 | 36.25 | 5.71 | 50 | 10 | 22.35 |
| Current investigation Unsteady, $Re = 3.40580\times10^5$, Condition 1, Avg. | 35 | 25.56 | 24.44 | 25.56 | 40 | 11.43 | 116 | 7.14 | 35.64 |

## 5. Conclusions

The primary purpose of this effort was to numerically simulate the wind flow around a U-section and to present the surface pressure coefficients distribution of different elements of the section at zero wind angles. Compared with general wind tunnel test, numerical simulation gives both real and ideal flow field distribution with lower cost and shorter time.

Results demonstrated that separation and recirculation regions develop wash away; resulting in down-wind flows, and then the circulation zone develops. The results indicate that the flow is up-down symmetrical for low values of oncoming Reynolds number and unsymmetrical for high values of on coming Reynolds number.

## Acknowledgments

This work was funded by the Deanship of Scientific Research (DSR), King Abdulaziz University, Jeddah, under grant No. (829-014-D1434). The authors, therefore, acknowledge with thanks DSR technical and financial support.

***Corresponding author:**
**Prof.** Walid A. Aissa
Faculty of Engineering at Rabigh, King Abdulaziz University, KSA, Permanent address: Mech. Power Dept., Faculty of Energy Engineering, Aswan UniversityAswan, Egypt.
Email: walidaniss@gmail.com

9/20/2013

## References

[1] Yuan W, Zhou H, Yao J, Xie J. Numerical simulation research on the aerodynamic performance of concavebuilding section. Procedia Engineering 2012;31: 206-212.
[2] Blocken B, Stathopoulos T, Saathoff P, Wang X. Numerical evaluation of pollutant dispersion in the built environment: comparisons between models and experiments. Journal of Wind Engineering and Industrial Aerodynamics 2008; 96: 1817-1831.
[3] Lien F S, Yee E, Cheng Y. Simulation of mean flow and turbulence over a 2D building array using high-resolution CFD and a distributed drag force approach. Journal of Wind Engineering and Industrial Aerodynamics 2004; 92: 117–158.
[4] Chang C H, Meroney R N. Concentration and flow distributions in urban street canyons: wind tunnel and computational data. Journal of wind Engineering and Industrial Aerodynamics 2003; 91: 1141-1154.
[5] Leitl B M, Kastner-Klein P, Rau M, Meroney R N. Concentration and flow distributions in the vicinity of U-shaped buildings: Wind-tunnel and computational data. Journal of wind Engineering and Industrial Aerodynamics 1997; 67&68 :745-755.
[6] Chang C H, Meroney R N. Numerical and physical modeling of bluff body flow and dispersion in urban street canyons. Journal of wind Engineering and Industrial Aerodynamics 2001; 89: 1325-1334.
[7] He J, Song C C S. A numerical study of wind flow around the TTU building and the roof corner vortex. UMSI 96/160, August 1996.
[8] Moroney R N, Leitl B M, Rafailidis S, Schatzmann M. Wind-tunnel and numerical modeling of flow and dispersion about several building shapes. Journal of Wind Engineering and Industrial Aerodynamics 1999; 81: 333-345.
[9] Kastner-Klein P, Plate E. Gaseous pollutant dispersion around urban-canopy elements: wind-tunnel case studies. Int. J. Environment and Pollution 1997, 8(3-6): 727-737.
[10] Norris, S. E. and Richards, P. J., "Appropriate boundary conditions for computational wind engineering models revisited," The Fifth International Symposium on Computational Wind Engineering (CWE2010), USA, May 23-27, 2010.